GEOMAGNETIC FIELD, GLOBAL PATTERN

Definition
The geomagnetic field is the Earth's magnetic field and in this chapter we describe how its pattern is mapped at the surface of the Earth through time.

Introduction
The geomagnetic field is generated in the fluid outer core region of the Earth by electrical currents flowing in the slowly moving molten iron. In addition to sources in the Earth's core the geomagnetic field observable at the Earth's surface has sources in the crust and in the ionosphere and magnetosphere. The signal from the core dominates, accounting for over 95% of the field at the Earth's surface. The geomagnetic field varies on a range of scales, both temporal and spatial; the description of the variations made here concentrates on the recent spatial and temporal variations of the field with origins in the Earth's core that can be surmised from observations made over the last four centuries.

Observations
The geomagnetic field is a vector quantity, having magnitude as well as direction. The direction of the geomagnetic field has been directly observed and recorded for at least 400 years beginning with observations of the angle in the horizontal plane between true north and the magnetic field vector, known as declination or magnetic variation. In 1634 it was realised by Henry Gellibrand that declination in London was changing with time when he compared his observations with those made by Edmund Gunter 12 years earlier. Since then this important discovery of secular variation has ensured regular observations of the magnetic field through time. Measurements of declination were important for navigation across the oceans, and a source of early observations is ships' logbooks (Jackson *et al*, 2000). Before long it was also realised that other elements of the geomagnetic field were of interest, in particular the angle of dip of the magnetic field vector from the horizontal known as inclination, and this was also measured. However it was not till 1832 when Carl Freidrich Gauss established his technique for measuring absolute intensity did we have accurate measurements of the magnitude of the geomagnetic field.

As demands on accuracy and interest in the geomagnetic field increased, permanent observatories began to be established. Since the 1840s the number of observatories around the world has slowly increased to a peak of about 180 in the late 1980s and early 1990s but is about 160 in recent times. The advent of the proton precession magnetometer and the fluxgate magnetometer in the 20th century considerably eased the automation of observatories during this time. However regular manual absolute observations, nowadays of declination and inclination using a fluxgate theodolite, are necessary to maintain accurate baseline control over long periods of time. There are also networks of repeat stations providing data over extensive areas from which country-wide magnetic charts could be derived. More recently, magnetic measurements made by satellites have become important in determining the pattern of the geomagnetic field. In particular, vector data from Magsat (1979-1980), Ørsted (1999-2013), CHAMP (2000-2010) and Swarm (2013-) have all been utilised in the production of recent spherical harmonic models of the geomagnetic field.

Spherical harmonic analysis
Till the 1950s magnetic charts at a given epoch for use in navigation depended on manually drawing contours through the observations (Malin, 1971). Although spherical harmonic analysis had been developed in 1839 by Carl Freidrich Gauss it was not routinely used to fit mathematical models to the observations till the advent of computers. Before computers spherical harmonic analysis required that the data be in the form of values of one or more of the orthogonal components X, Y and Z of the geomagnetic field (magnetic intensities in the northerly, easterly and vertically down directions) at points regularly spaced in latitude and longitude (Barraclough,

1978). This involved the intermediate stage of interpolating values from manually drawn contour charts.

The mathematical and physical basis for spherical harmonic analysis is now given. In a source-free region the Earth's magnetic field **B** is the negative gradient of a magnetic potential V that satisfies Laplace's equation:

$$\mathrm{B} = -\nabla V \quad \text{where} \quad \nabla^2 V = 0$$

A solution to Laplace's equation for the magnetic potential arising from sources inside the Earth at a given epoch is given by:

$$V(r,\theta,\lambda) = a\sum_{n=1}^{n_{\max}} \left(\frac{a}{r}\right)^{n+1} \sum_{m=0}^{n} \left(g_n^m \cos m\lambda + h_n^m \sin m\lambda\right) P_n^m(\theta)$$

In this equation r, θ, λ are geocentric coordinates (r is the distance from the centre of the Earth, θ is the colatitude, i.e. 90° - latitude, and λ is the longitude), a is a reference radius for the Earth (6371.2 km), g_n^m and h_n^m are the spherical harmonic Gauss coefficients of degree n and order m, $P_n^m(\theta)$ are the Schmidt semi-normalised Legendre functions and n_{max} is the maximum degree of the spherical harmonic expansion. If the observations of the magnetic field are spread over time, the magnetic potential and corresponding Gauss coefficients are also dependent on time with splines being commonly used.

Maps of the geomagnetic field

It is worth noting here that the first published map of the geomagnetic field is that of declination made in 1701 by Edmond Halley. It was based on declination observations made during a magnetic survey expedition under naval command and covered the Atlantic Ocean (Clark & Barraclough, 2001).

The maps that we show here are based on spherical harmonic models. Nowadays there are many such models of the geomagnetic field and here we look at two examples. One is the *gufm1* model which is derived from four centuries of magnetic field observations (Jackson *et al*, 2000) and extends to spherical harmonic degree 14 with B-splines being used to fit the variations in time from 1590 to 1990. It has smoothness imposed in both the spatial and temporal domains. The other model is the International Geomagnetic Reference Field (Thébault *et al*, 2015) produced under the auspices of the International Association of Geomagnetism and Aeronomy (IAGA). It extends to spherical harmonic degree 10 till 1995 and thereafter extends to degree 13. The variations in time from 1900 to 2020 in the IGRF are assumed to be piecewise linear and there is effectively no smoothness imposed in either the spatial or temporal domains. The final IGRF coefficients are made up of weighted averages of candidate sets of coefficients from (mostly) unregularized models.

Using the *gufm1* model, plots of declination and inclination at 1600, declination, inclination and total intensity at 1950 are shown in Figures 1 and 2. Using the 12th generation IGRF, plots of the magnetic elements at 2015 and their rates of change are shown in Figures 3-9. The rates of change plots are derived from a predictive secular variation model which extends to spherical harmonic degree 8. Up-to-date maps, and on-line calculators are available from a number of websites, for example https://geomag.bgs.ac.uk/navigation.html and https://ngdc.noaa.gov/geomag/WMM/DoDWMM.shtml.

Figure 1 Declination and inclination at 1600.0 (degrees) computed from the *gufm1* model

Figure 2 Declination, inclination (degrees) and total intensity (nT) at 1950.0 computed from the *gufm1* model

Figure 3 Northerly intensity (nT) at 2015.0 and its rate of change (nT/year) for 2015.0-2020.0 computed from IGRF-12

Figure 4 Easterly intensity (nT) at 2015.0 and its rate of change (nT/year) for 2015.0-2020.0 computed from IGRF-12

Figure 5 Vertical intensity (nT) at 2015.0 and its rate of change (nT/year) for 2015.0-2020.0 computed from IGRF-12

Figure 6 Horizontal intensity (nT) at 2015.0 and its rate of change (nT/year) for 2015.0-2020.0 computed from IGRF-12

Figure 7 Declination (degrees) at 2015.0 and its rate of change (arc-minutes/year) for 2015.0-2020.0 computed from IGRF-12

Figure 8 Inclination (degrees) at 2015.0 and its rate of change (arc-minutes/year) for 2015.0-2020.0 computed from IGRF-12

Figure 9 Total intensity (nT) at 2015.0 and its rate of change (nT/year) for 2015.0-2020.0 computed from IGRF 12

Features of note on these maps are the dip equator and dip poles in the maps of inclination (Figures 1, 2 and 8) and the area of weak magnetic field in the South Atlantic, and strong magnetic field near the poles in Figures 2 and 9. The dip equator is where the magnetic field is horizontal (inclination = 0°) and a current system is set up in the upper atmosphere called the equatorial electrojet. The dip poles (also called magnetic poles) are locations where the magnetic field is, on average, vertical. Another set of poles is the dipole poles or geomagnetic poles. Their positions can be derived from the degree 1 spherical harmonic coefficients (g_1^0, g_1^1 and h_1^1). Associated with the geomagnetic poles, in approximately oval shaped loci, are the auroral electrojets in the upper atmosphere. The electrojets, particularly the auroral electrojets, generate rapid time-varying magnetic fields of significant amplitude.

Recent changes in the geomagnetic field

From a comparison of the declination maps in Figures 2 and 7 it can be seen that the zero contour (the agonic line) is moving slowly westwards with time. This westwards movement of the magnetic field pattern at the Earth's surface, particularly prevalent in the Atlantic hemisphere, is related to the motion of fluid at the core surface slowly westwards, dragging with it the magnetic field lines.

At high northern latitudes from 2000 to 2020 the motion of the north dip pole has been more than 50 km per year and sometime during 2017/2018 it reached its highest latitude (86.6°N). According to the latest IGRF we are now seeing a deceleration of this motion, but the pole is still moving at roughly 40 km per year, and heading southwards. In contrast, the southern dip pole, near Antarctica, has moved relatively little in the past few hundred years.

Using IGRF-12 to compute the root mean square magnetic field vector at the Earth's surface arising from all spherical harmonic terms ($n \leq 10$), the centred dipole terms ($n = 1$) and the non-dipole terms ($1 < n \leq 10$), it can be seen in Figure 10 that since 1900 the geomagnetic field is weakening overall by becoming less dipolar. However the non-dipolar part is strengthening. This may have consequences for the trajectories of energetic charged particles that enter the Earth's magnetosphere. One manifestation of this is the deepening, and westwards movement, of the South Atlantic Anomaly, the region where the geomagnetic field is weaker than elsewhere (see Figures 2 and 9). Energetic charged particles are able to penetrate closer to the Earth and cause a radiation hazard for satellites passing through this region.

Figure 10 Decline of the whole, and dipolar part of the geomagnetic field at the Earth's surface and the growth of the non-dipolar part since 1900, computed from IGRF-12

Superimposed on these gradual changes of the magnetic field are the so-called geomagnetic jerks. They are relatively abrupt (duration of months) changes in the second time derivative, or secular acceleration, of the magnetic field. The first observed geomagnetic jerk was that around 1969, and since the late 19th century when direct and continuous measurements of the Earth's magnetic field have been available, geomagnetic jerks have also been widely accepted to have occurred around 1925, 1978 and 1991. These jerks are most readily observed in the first time derivative of the easterly intensity at European observatories (Figure 11). More recent jerks are also being detected, sometimes with help of data from satellites.

Figure 11 Geomagnetic jerks as seen in the secular variation of the east component of the geomagnetic field observed at European observatories. Times of jerks are shown by arrows.

Various analysis techniques have been applied to jerks to investigate specific aspects of their temporal and spatial characteristics. For example Brown *et al* (2013) used minimal *a priori* information to accurately time the occurrence of jerks around the world and establish their amplitudes using observatory data. The variable timing is particularly interesting for studies of the geodynamo though the effects of varying conductivity in the deep mantle on the arrival time of the jerk signals at the Earth's surface cannot be discounted (Pinheiro *et al*, 2015). Understanding the origin of jerks is also important for improving time-dependent models of the geomagnetic field and for the strictly practical purpose of forecasting its future behaviour, for example, as used in navigation and orientation.

Summary

In this chapter we have described the global mapping of the geomagnetic field for the 400+ year period during which direct field observations have been available. The mapping technique involving the fitting of spherical harmonic models is described, and maps of the various components of the magnetic field are provided for 1600, 1950 and the present day. The geomagnetic field is constantly changing on a range of temporal and spatial scales and these changes provide scientists with important information about processes deep inside the Earth.

Susan Macmillan

Cross references

Geomagnetic field, IGRF

Geomagnetic field, secular variation
Geomagnetic field, measurement techniques
Geomagnetic field, theory
Global Magnetic Anomaly Map
Magnetic methods, satellite

References

Barraclough, D. R., 1978. Spherical harmonic models of the geomagnetic field. *Geomagnetic Bulletin Institute of Geological Sciences*, No. 8.

Brown, W.J., Mound, P.W. and Livermore, P.W., 2013. Jerks abound: an analysis of geomagnetic observatory data from 1957 to 2008, *Phys. Earth planet. Int.*, 223, 62–76.

Clark, Toby and David Barraclough, 2001. The first magnetic chart, *Astron. Geophys*. 42, 1.23-1.25.

Malin, S. R. C., 1971. British World Magnetic Charts. *IAGA Bulletin* No. 28, World Magnetic Survey 1957-1969. Ed. A. J. Zmuda.

K. J. Pinheiro, A. Jackson and H. Amit, 2015. On the applicability of Backus' mantle filter theory. *Geophys. J. Int.*, 200, 1336–1346.

Thébault *et al*, 2015. International Geomagnetic Reference Field: the 12th generation. *Earth, Planets and Space*, 67-79, https://doi.org/10.1186/s40623-015-0228-9.

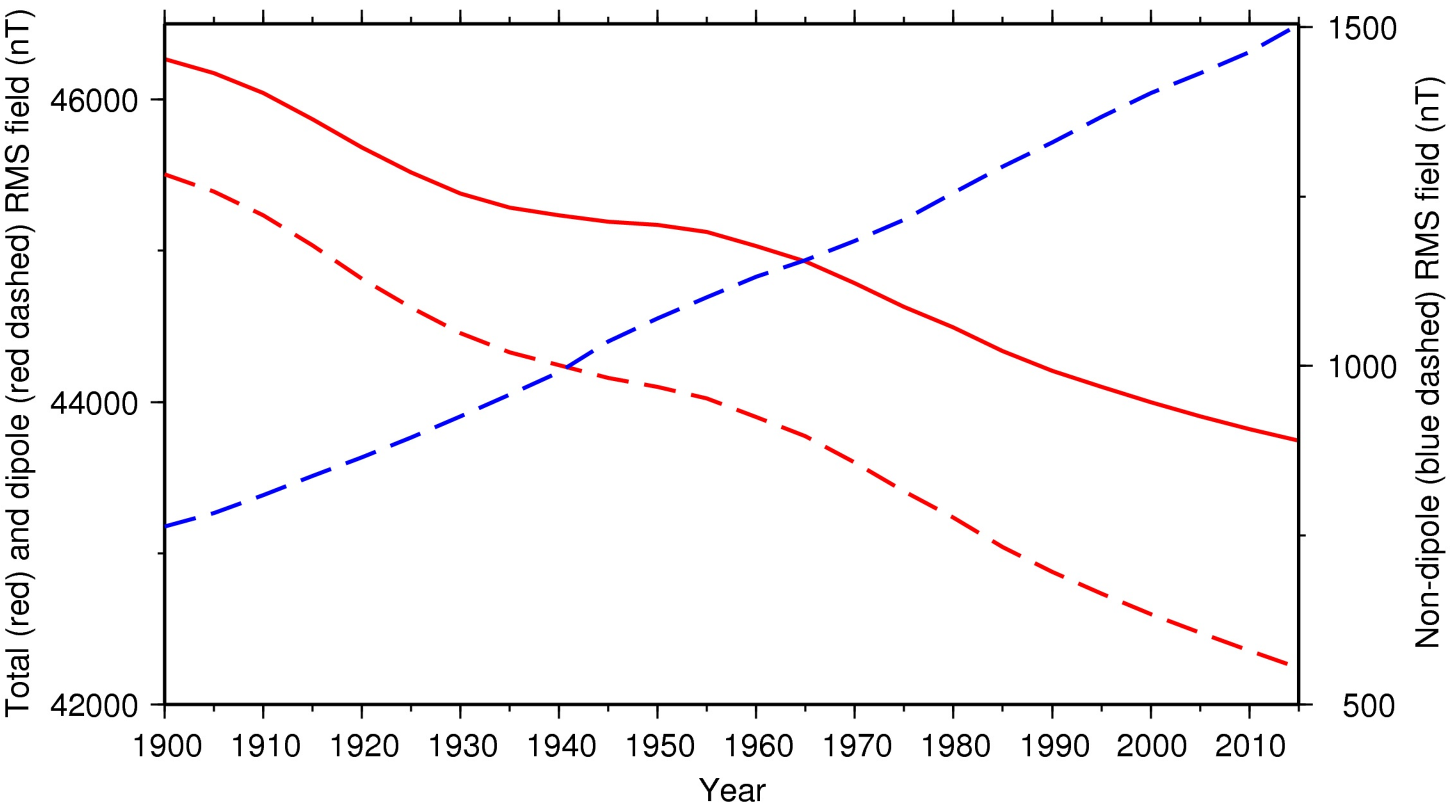

Total (red) and dipole (red dashed) RMS field (nT)
46000
44000
42000
1900
1910
1920
1930
1940
1950
1960
1970
1980
1990
2000
2010
Year
1500
1000
500
Non-dipole (blue dashed) RMS field (nT)